frontiers | Frontiers in Plant Science

TYPE Original Research
PUBLISHED 05 December 2023
DOI 10.3389/fpls.2023.1247169

Check for updates

OPEN ACCESS

EDITED BY
Lei Shu,
Nanjing Agricultural University, China

REVIEWED BY
Yuanhao Sun,
Jiangsu Academy of Agricultural Sciences (JAAS), China
Tariq Mukhtar,
Pir Mehr Ali Shah Arid Agriculture University, Pakistan

*CORRESPONDENCE
Jiyu Li
lijiyu@scau.edu.cn

RECEIVED 25 June 2023
ACCEPTED 20 November 2023
PUBLISHED 05 December 2023

CITATION
Xing H, Li M, Qin Y, Fan G, Zhao Y, Lv J and Li J (2023) Design of a trichogramma balls UAV delivery system and quality analysis of delivery operation.
Front. Plant Sci. 14:1247169.
doi: 10.3389/fpls.2023.1247169

COPYRIGHT
© 2023 Xing, Li, Qin, Fan, Zhao, Lv and Li. This is an open-access article distributed under the terms of the Creative Commons Attribution License (CC BY). The use, distribution or reproduction in other forums is permitted, provided the original author(s) and the copyright owner(s) are credited and that the original publication in this journal is cited, in accordance with accepted academic practice. No use, distribution or reproduction is permitted which does not comply with these terms.

Design of a trichogramma balls UAV delivery system and quality analysis of delivery operation

Hang Xing, Mengjie Li, Yijuan Qin, Gangao Fan, Yinwei Zhao, Jia Lv and Jiyu Li*

College of Engineering, South China Agricultural University, Guangzhou, China

The field boundaries in our country are complex. In attempts to control pests via trichogramma-dominated biological control, the long-term practice of manual trichogramma release has resulted in low control efficiency, thereby impeding sustainable agricultural development. Currently, the novel approach involves utilizing Unmanned Aerial Vehicles (UAVs) for trichogramma balls delivery; however, the system is still in its nascent stages, presenting opportunities for enhancement in terms of stability and accuracy. Furthermore, there is a notable absence of comprehensive operational quality assessment standards. In this study, we establish a stable and accurate trichogramma balls delivery system using a four-axis plant protection UAV and introduce a comprehensive evaluation method for trichogramma balls delivery system. When dealing with fields with complex boundaries, it is beneficial to divide them into rectangular, trapezoidal, and stepped small fields at the boundary and perform operations within these small fields. According to our proposed evaluation method, when only considering the effect of field operations, the most effective boundary division shape is trapezoidal, followed by rectangular. and the worst is stepped. If both field operation effectiveness and the utilization effect of placed trichogramma balls are considered, the optimal shape is trapezoidal, then stepped, with rectangular being the least effective. Consequently, for UAV sub-area operations in complex boundary fields, it is advisable to divide the boundaries into trapezoids wherever possible. Field experiment results indicate that the system's delivery area can reach up to 4158 m^2/min and the coverage rate of released trichogramma balls can exceed 97%. The system design methodology and comprehensive operational quality evaluation method proposed in this article provide technical support and scientific basis for the application and promotion of UAV delivery trichogramma balls system. This is conducive to the high-quality development of agriculture.

KEYWORDS

UAV, trichogramma ball, delivery system, operational quality, biological control

1 Introduction

In global agricultural production, agricultural pests are one of the key factors leading to food loss, causing significant economic losses to the development of agriculture. The long-term use of chemical pesticides in the current pest control process has led to resistance in field populations to commonly used pesticides; insecticides also pose problems such as killing natural enemies, causing pesticide residues and water pollution, which restrict the sustainable development of agriculture (Cheng and Zhu, 2017). Therefore, in order to ensure the safety of agricultural production and achieve sustainable development in the long run, the methods of pest control need to be transformed.

With the enhancement of people's awareness of environmental protection and the continuous development of green agriculture, biological control methods are replacing traditional pesticide control and have become an important means for the green prevention and control of crop pests (Gauthier et al., 2019; Kumar and Arthurs, 2021). Biological control is mainly to put natural enemies of crop pests in the field, so that a large number of them are scattered in the field, so as to use parasitic, predation and other methods to reduce the number of pests, thereby reducing food loss and improving crop quality (Wang et al., 2019). This method is environmentally friendly and pollution-free while protecting agricultural products. Trichogramma species make up one of the most commonly used groups of natural enemies for biological control programs worldwide (Babendreier et al., 2019; Zang et al., 2021), they have a wide range of hosts, a wide distribution range, and a fast reproduction rate, then play an important role in disease and pest control of rice, corn, sugarcane, vegetables and some trees (Xu et al., 2016). At present, the main methods of releasing trichogramma include manual spraying trichogramma suspensions, manual hanging trichogramma cards, and manual delivering trichogramma releasers, etc. It is difficult to achieve the expected goals in terms of uniformity, coverage, and delivery speed using this long-term manual delivery method. At the same time, there is a significant lag in the strong timeliness of biological control, and the high labor cost also hinders the widespread use of this method.

In recent years, with the continuous development of agricultural machinery, mechanized equipment that can be used to deliver trichogramma is gradually emerging, mainly including ground equipment and aviation equipment.

The ground equipment mainly adopts air blowing to drop carriers carrying trichogramma or to spray trichogramma suspensions. Giles et al. designed an air blown delivery device installed on tractors after multiple improvements, the device included a storage container, a rotating metering plate, and an air-cleared ejection port. As the metering plate rotated, the formulation filled cylindrical cells in the plate. As the filled cells passed an opening on a stationary bottom plate, the cell contents fell downward while a brief pulse of compressed air insured that each cell was cleared. Release rate of the mites was controlled through rotational speed of the metering plate and the size of cells on the plate. In laboratory and field tests, this method will not disrupt the activity of natural enemies. The implementation of this method has significantly enhanced operational efficiency (Giles et al., 1995). Dionne et al. designed and tested a boom sprayer to spray trichogramma ostriniae in sweet corn canopy under real field conditions. The sprayer was equipped with a 380L water tank, and 8 XR11008-VP nozzles were installed on a 6.71m spray rod. A diaphragm pump with a flow rate of 18.5L/min was used for pressure supply. During operation, the equipment was mounted on tractors or other implements. Field trial results showed that spraying was 1.7 times faster than the manual introduction of Trichocards, and the results indicated that spraying is a promising technique for an efficient and viable introduction of parasitized eggs (Dionne et al., 2018). The above research has proven that the efficiency of using ground equipment to release Trichogramma is higher. However, the control mechanism of trichogramma determines that it needs to be placed multiple times during the crop growth cycle. The ground machine entering the field multiple times can easily compact the soil, and it has poor trafficability in fields with tall crops, making it unsuitable for operations in late stages of crop growth such as corn. As a result, some researchers began to investigate the use of aviation equipment to delivery trichogramma. Aviation equipment mainly includes manned aircraft and UAVs.

In terms of using manned aircraft, An automatic insect release system (AIRS) was developed by the International Institute of Tropical Agriculture in collaboration with Firma Dieringer of Austria and Ciba-Pilatus (now Zimex Aviation) of Switzerland for the aerial distribution of natural enemies of two cassava pests. The AIRS, installed in a twin turbo-prop aircraft, had undergone a series of tests to evaluate suitable packaging substrates, pre- and post-release mortality, biological performance and ground distribution of natural enemies (Herren et al., 1987). Bzowska-Bakalarz et al. attempted to use the Aviation Artur Trendak Zen-1 ultra light rotorcraft to control corn borers in farmland. They installed trichogramma dispensers at both ends of the fuselage rack, with a single operational area up to 80hm^2 and a flight speed up to 100km/h, and several years of field application have shown that the prevention effect against corn borers has reached 60% to 85% (Bzowska-Bakalarz et al., 2020). The above method of using manned aircraft for operation is not only efficient, but also does not contact with crops and the ground, so can be used as a good supplement to the ground delivery machinery. However, it has high cost, high flight speed and altitude, large operating width, large turning radius, and is not suitable for complex small plot operations.

Unmanned aerial vehicles can effectively solve the problem of poor trafficability in tall stalk crop fields and soil compaction by traditional ground machinery. Compared to manned aircraft, UAVs have the advantages of small size, easy use, no need for special take-off runways, low cost, and greater promotion potential, which makes them promising for a wide range of applications (Parra, 2014; Yang et al., 2019; Chen et al., 2020; Iost et al., 2020). Li et al. applied drone technology to the delivery of trichogramma, and sprayed the egg suspension of trichogramma by peristaltic pump under pressure through the UAV spraying system. The test proved that spraying trichogramma eggs with plant protection drones had no significant effect on its activity (Li et al., 2013). Xu et al. conducted a release test of trichogramma using a six-axis multirotor UAV. Their test results showed that the coverage rate of the trichogramma deployed reached 100%, with an average

hatching rate of 75.81%. However, there was a lack of analysis on the actual field coverage rate and the overall quality of field operations (Xu et al., 2016). Martel et al. used Entobot biological delivery aircraft to drop trichogramma in the forest, the experimental results showed that compared with manual delivery, UAV delivery cost was higher, but delivery was rapid and a lot of time was saved, and the control effect of the two methods was almost the same (Martel et al., 2021). Zhan et al. carried out the field delivery test based on the M45 UAV equipped with special ground station, sky station and mobile phone client, they realized the functions of path planning, recording the coordinates of the delivery point and generating operational map. The actual coverage of the test site reaches 99.33%, which can meet the operational requirements (Zhan et al., 2021). Although a lot of research has already been done, in order to further improve the field operational quality of UAVs for biological control, the stability and delivery accuracy of UAVs carrying and releasing insect systems need to be improved, and the comprehensive operational quality evaluation method needs to be clarified.

At the same time, the shape of natural farmland in China is affected by climate, terrain, water source and other factors, and most of them exhibit complex boundaries. As shown in Figure 1, the complex boundaries of the field are marked with red lines, and the basic polygons in the field are marked with yellow lines. During the operation of UAVs, the entire field will be divided into several small fields for operation. So the operational quality and efficiency in each small field will become the main factors affecting the comprehensive operational quality of UAVs.

In this article, we designed a new trichogramma balls delivery system based on a four-axis multirotor UAV, independently designed its delivery device and control system, completed the stability and accuracy analysis of the system and its operational efficiency tests in various field plots, especially proposed a comprehensive operational quality evaluation system to evaluate the results of field trials of the system, and pointed out which shape should be divided at the boundary when dividing complex boundary fields from the perspective of improving the comprehensive operational quality.

2 Materials and methods

2.1 Design of the trichogramma balls delivery system

The trichogramma balls delivery system is built using a quad-rotor unmanned plant protection aircraft (EFT E410S) and a flight control system (JIYI K++). The structure is shown in Figure 2. The drone has a maximum operating height of 50m, a maximum speed of 10m/s, and a maximum takeoff weight of 25kg. The main frame is made of carbon fibre material. The folding arms are symmetrically mounted on the two diagonal lines of the frame using injection molding technology. A motor is installed at the end of the arm (Zhan et al., 2021; Ji et al., 2022).

The ground control system includes BeiDou mobile station, base station, and upper computer to obtain real-time information on flight altitude, speed and trajectory parameters of the drone during operation, as well as the actual landing point location information of the trichogramma balls. The structural diagram is shown in Figure 3. The core module of the system is the BeiDou board card (ComNav K705), with detailed technical parameters shown in Table 1. A data transmission module (Microhard P900) is used as the Beidou data wireless transmission device.

The trichogramma ball is made of degradable composite material using injection moulding technology. The trichogramma eggs are loaded inside the trichogramma ball, which can avoid the trichogramma from being exposed to the outside world before eclosion. The shape of the trichogramma ball is like a cylinder, with a diameter of 18 mm and a height of 18 mm, the edges of both ends are rounded with a radius of 5 mm, and the maximum diameter length is 20.5 mm, this structure can prevent the trichogramma ball from rolling too far after falling to the ground. There are eight breathable holes on both ends with a diameter of 0.5 mm, preventing natural enemies from swallowing insect eggs while ensuring a certain degree of breathability. The structure of the trichogramma ball is shown in Figure 4.

The delivery device mainly includes a base, material bucket, balls distribution plate, stirring connecting piece, stirring sphere,

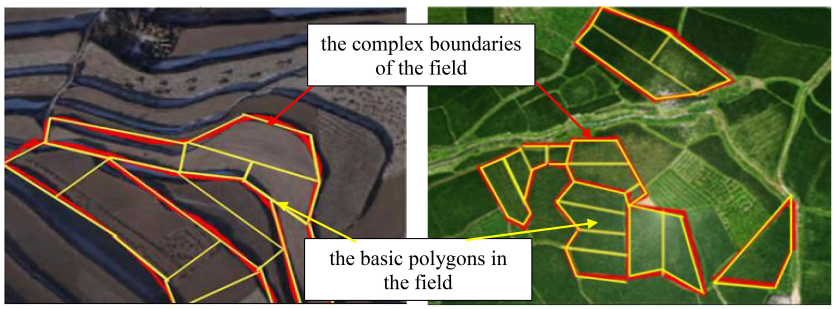

FIGURE 1
Map of natural fields with complex boundaries.

10.3389/fpls.2023.1247169

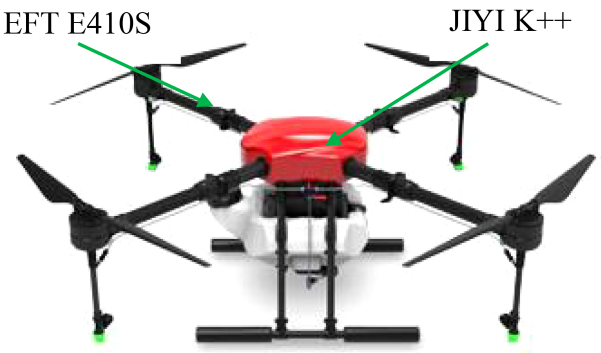

FIGURE 2
The structure diagram of the trichogramma balls UAV delivery system.

and steering engine, as shown in Figure 5. The base matches the bottom of the material bucket, the four pits in the inner circle correspond to the protrusions around the bottom hole of the material bucket, two circular tracks are designed on the base, then the entering balls can slide along the tracks, ensuring that the balls can fall into the balls distribution plate at any posture. After the steering engine is installed on the base, the steering plate is sequentially connected with the balls distribution plate, the stirring connecting piece and the stirring sphere through bolts.

The circuit part of the control system of the trichogramma balls delivery device is composed of three parts: the power module (LM2596HVS step-down module), the control module (STM32F103C8T6), and the output module (DS3230 360° metal digital rudder). These components are directly connected to the UAV flight control system to realize the matching of the UAV flight speed and the trichogramma balls delivery speed. That is, the distance between trichogramma balls released at any flight speed is always a fixed value, so as to avoid the problem of uneven delivery of the balls in the field and achieve the linkage effect. The steering engine rotates when the PWM signal is input, so the speed of the

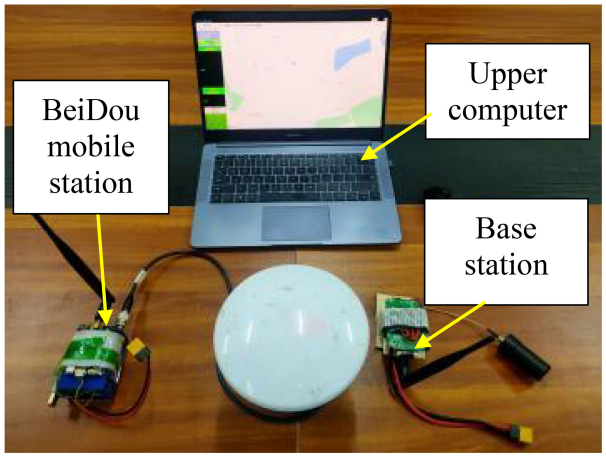

FIGURE 3
Ground control system.

TABLE 1 Technical Parameters of K705 Board.

Technical parameter	Parameter value
Single point positioning accuracy	H<1.5 m, V<3 m (1δ, PDOP<4)
Static differential accuracy	H: ±(2.5 + 1×10^{-6}×D) mm V: ±(5.0 + 1×10^{-6}×D) mm
RTK accuracy	H: ±(8.0 + 1×10^{-6}×D) mm V: ±(15 + 1×10^{-6}×D) mm
Timing accuracy	20 *ns*

steering engine is tested under different PWM input signals, and the functional relationship between the PWM signal value $x_1(\mu s)$ (input to the steering engine and the steering engine speed n(r/min) obtained by fitting is shown in Equation 1, the determination coefficient $R^2 = 0.9968$.

$$n = \frac{x_1 - 1495.5}{22.802} \tag{1}$$

The steering engine rotates 1/3 of a turn to drop a trichogramma ball and the UAV is required to put the trichogramma balls at equal intervals l(m), the UAV flight speed v(m/s) and the steering engine speed n(r/min) meet the Equation 2:

$$n = \frac{1}{3}\frac{60v}{l} = \frac{20v}{l} \tag{2}$$

Therefore, the relationship between the PWM signal value x_1 (μs) input to the steering engine and the UAV flight speed v(m/s) can be expressed as follows:

$$x_1 = 456.04\frac{v}{l} + 1495.5 \tag{3}$$

Through flight test, the relationship between PWM value $x_2(\mu s)$ of flight controller output and UAV flight speed v(m/s) can be obtained as follows:

$$x_2 = 83.333v + 1000 \tag{4}$$

Then the PWM value $x_2(\mu s)$ of flight controller output and the PWM signal value $x_1(\mu s)$ input to the steering engine should meet the following relationship:

$$x_1 = (x_2 - 1000)\frac{5.473}{l} + 1495.5 \tag{5}$$

2.2 Performance test of the trichogramma balls delivery system

In the actual field operations of UAVs, the mechanical structure stability and control system accuracy of the trichogramma balls delivery system will directly affect the quality of field operations of the system. Therefore, experiments were conducted on system stability and release accuracy.

The test site was located at the Qilin District Sports Ground of South China Agricultural University (23.15°N 113.35°E). The test was conducted under the conditions of sunny weather, no wind, and 28°C temperature. Each time, 200 balls were placed in the material bucket,

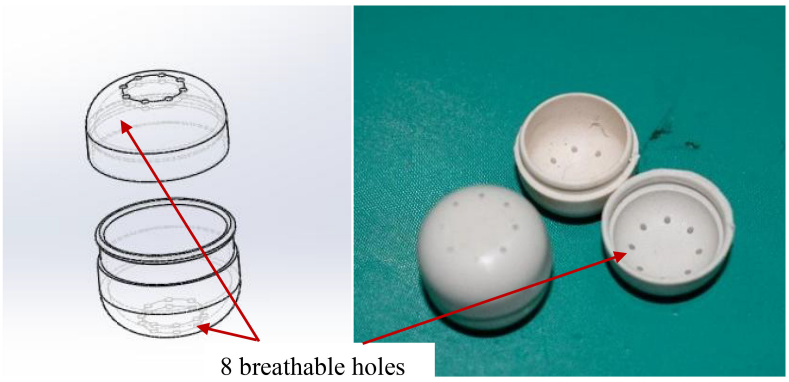

FIGURE 4
The structure of the trichogramma ball.

and five steering speeds of 6 m/s, 9 m/s, 12 m/s, 15 m/s and 18 m/s are set up through the delivery device control system. Three repeated releasing experiments are conducted respectively, and the number of balls released and the number of blocked and missed balls within two minutes were recorded, as shown in Table 2.

As can be seen from Table 2, when the steering speed is 6 r/min, 9 r/min, 12 r/min, 15 r/min and 18 r/min, the device's accuracy rate for releasing within 2 minutes reaches over 97.69%. Moreover, under these five speeds, all loaded balls are released without any issues of stuck balls or missed releases, indicating that the mechanical structure of this device is stable and reliable in releasing balls.

The trials conducted for the accuracy of system deployment in flight linkage mode includes two flight trajectories, each 80m long and 10m apart, with the UAV flight altitude set at 5m, UAV speeds are set to 3 m/s, 5 m/s, 7 m/s, and 9 m/s (Zhan et al., 2021). After each trial was completed, a tape measure was used to manually measure the distance between two adjacent balls on the same flight route (excluding acceleration and deceleration intervals). The actual landing site spacing data of the trichogramma balls under the four UAV flight speeds were recorded, and A One-way ANOVA (α = 0.05) was conducted using IBM SPSS (26.0) software. This study explored the impact of changes in UAV flight speed on the distance between the actual deployments of trichogramma balls, obtaining data in Table 3 (Ding et al., 2021; Fang et al., 2022; Wang et al., 2022).

As can be seen from Table 3, when the test level is α = 0.05, the F test falls in the acceptance range, sig. = 0.874 > 0.05, which indicates that the change in UAV flight speed do not have a significant impact on the actual landing site spacing between adjacent balls. Moreover, as shown in Table 3, the average spacing between adjacent balls is between 10.0 m and 10.5 m at the above four flight speeds. This proves that UAV's flight control can accurately coordinate with the delivery device to drop balls at the set spacing, and the release process is accurate and reliable.

2.3 Field operational quality evaluation test

The natural crop fields in our country often present complex boundaries, as shown in Figure 6. If the red lines are used to indicate the shape of the complex boundary of the field in the figure, and the yellow lines are used to indicate the basic polygons in the field, it can be seen that except for the largest rectangular field in the center of the field, any irregular field at the boundary position can be deconstructed from rectangular, trapezoidal, and stepped fields. The operational quality at the boundary position is an important factor affecting the overall operational quality of the entire field.

To explore the influence of rectangular, trapezoidal and stepped boundary fields on the overall field operational quality, a field

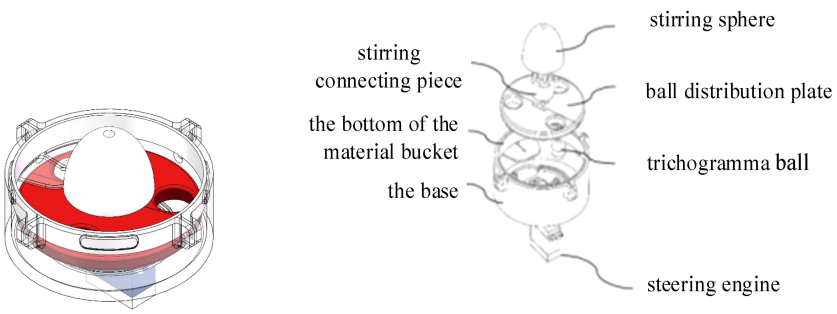

FIGURE 5
Delivery device structure.

TABLE 2 Number of released balls.

Steering engine speed (r/min)	Number of balls released within 2 minutes				Total number of balls released	Total number of blocked and missed balls
	Group 1	Group 2	Group 3	precision (%)		
6	36	35	36	99.07%	200	0
9	53	54	54	99.38%	200	0
12	74	74	73	97.69%	200	0
15	91	92	92	98.15%	200	0
18	108	109	108	99.69%	200	0

operation test of the trichogramma balls delivery system was carried out, as shown in Figure 7. The test site was located in a pineapple field at Guangken Agricultural Machinery in Zhanjiang, Guangdong (21.3°N 110.3°E). The rectangular, trapezoidal, and stepped fields with an area of approximately 8 acres were selected. The actual field area and boundary size of the three test plots were measured and marked on Figure 8, where the white line frame represented the boundary of the operational area, the red line represented the flight route of the UAV, the green circle marked with *S* represented the starting point of the UAV for releasing the balls, and the red circle marked with *F* represented the ending point of the UAV (Cao et al., 2020).

A trichogramma ball stores approximately 2000 trichogramma eggs, and the range of protection after the hatching of the contained trichogramma eggs is a circle with a diameter of 14.9 m centred on the trichogramma ball, as shown in the green circle in Figure 9. To achieve full coverage of the UAV operational area, the spacing L of the released balls should be less than or equal to 10.5 m , $(d/\sqrt{2})$ as shown in Figure 9, so the flight path spacing is set to 10.5 m. The flight speed is set to 7 m/s. After the test flight is completed, the mobile station is removed from the UAV and installed on a handheld fixture to make a ball landing point data sampler. The locations of the dropped balls were sampled one by one in the pineapple field, as shown in Figure 10.

2.4 Field operational quality evaluation method

In order to evaluate the actual field operational quality of the trichogramma balls UAV delivery system in linkage mode, an actual landing map was drawn based on the actual operational route and the landing point position, that is, the actual operational status was drawn in Auto CAD (2022). The target area S_0, effective coverage area S_1, uncovered area S_2, ineffective coverage area S_3, repetitive covered area S_4, and total coverage area S_n are defined as shown in Figure 11, and the operational performance indicators, effective coverage rate η_1, uncovered rate η_2, ineffective coverage rate η_3, utilization rate of balls η_4, and repetition rate of balls η_5, are also defined as follows.

The effective coverage rate η_1 meets Equation 6:

$$\eta_1 = S_1/S_0 \tag{6}$$

TABLE 3 Experimental and analytical data on the spacing of trichogramma balls placement.

Flight speed (m/s)	3		5		7		9	
	Route 1	Route 2	Route 1	Route 2	Route 1	Route 2	Route 1	Route 2
Spacing 1(m)	10.0	9.7	8.0	11.0	9.4	9.3	9.1	9.9
Spacing 2(m)	10.5	10.0	12.5	11.4	9.3	10.0	10.6	11.2
Spacing 3(m)	10.0	9.4	10.1	10.3	11.6	10.5	9.9	9.9
Spacing 4(m)	9.8	10.2	10.6	10.4	9.3	11.1	11.8	10.9
Spacing 5(m)	11.3	9.6	11.0	10.7	11.4	11.0	10.8	10.1
Spacing 6(m)	9.9	10.7	9.9	8.4	10.2	11.0	9.6	9.7
Average spacing(m)	10.3	10.0	10.4	10.4	10.2	10.5	10.3	10.3
Sum of squares	0.543							
Mean square	0.181							
F	0.231							
Sig.	0.874							

FIGURE 6
Natural field boundary diagram.

The uncover rate η_2 meets Equation 7:

$$\eta_2 = S_2/S_0 \tag{7}$$

The ineffective coverage rate η_3 meets Equation 8:

$$\eta_3 = S_3/S_0 \tag{8}$$

The utilization rate of balls η_4 meets Equation 9:

$$\eta_4 = S_1/(S_0 + S_3) \tag{9}$$

The repetition rate of balls η_5 meets Equation 10:

$$\eta_5 = S_4/S_n \tag{10}$$

The system operational indicators η_1,η_2,η_3,η_4,η_5, all affect the overall operational quality of the system, but the influence degrees of each are different, so the influence of each indicator needs to be reflected by weights. The entropy weight method is an objective weighting method for determining the weights of evaluation indicators. This method is based on the current sample data to obtain the weight of the indicators by statistics, avoiding deviations caused by human factors. The process of evaluating the overall operational quality using the entropy weight method is as follows (Qin et al., 2023):

1) Construct an evaluation indicator matrix $X = (x_{ij})_{mn}, i = 1, 2, \cdots, m; j = 1, 2, \cdots, n$. where x_{ij} represents the value of j-th indicator of the i-th sample. m represents the number of field types, and n represents the number of indicators.

2) Standardize the indicators. If the indicator has a positive effect (the larger, the better), the standardization method is as follows.

$$x_{ij}^{'} = \frac{x_{ij} - minx_{ij}}{maxx_{ij} - minx_{ij}}, i = 1, 2, \cdots, m; j = 1, 2, \cdots, n \tag{11}$$

If the indicator has a negative effect (the smaller, the better), the standardization method is as follows.

$$x_{ij}^{'} = \frac{maxx_{ij} - x_{ij}}{maxx_{ij} - minx_{ij}}, i = 1, 2, \cdots, m; j = 1, 2, \cdots, n \tag{12}$$

Where $x_{ij}^{'}$ is the standardized indicator value and represents the j-th standard indicator value of the i-th sample.

3) Use the translation method to handle special situations that may occur after standardization.

$$x_{ij}^{''} = H + x_{ij}^{'}, i = 1, 2, \cdots, m; j = 1, 2, \cdots, n\ H = 0.01 \tag{13}$$

4) Calculate the proportion matrix $P = (p_{ij})_{mn}$, where p_{ij} represents the proportion of the j-th indicator value of the i-th sample, and take it as the probability when calculating the information entropy.

$$p_{ij} = \frac{x_{ij}^{''}}{\sum_{i=1}^{m} x_{ij}^{''}}, i = 1, 2, \cdots, m; j = 1, 2, \cdots, n \tag{14}$$

5) Calculate the information entropy matrix of the evaluation indicators $E = (e_j)$. e_j represents the information entropy of the j-th indicator.

$$e_j = \frac{1}{\ln m} \sum_{i=1}^{m} p_{ij} I_{ij}, j = 1, 2, \cdots, n \tag{15}$$

Where $I_{ij} = -lnp_{ij}$ represents the information of the j-th indicator value of the i-th sample. The larger p_{ij} is, the smaller the uncertainty is, and the less information it contains. The maximum value of $\sum_{i=1}^{m} p_{ij} I_{ij}$ is lnm, so dividing $\sum_{i=1}^{m} p_{ij} I_{ij}$ by a constant lnm to make e_j falls between [0,1].

6) Calculate the evaluation matrix $W = (w_j)$. w_j represents the weight of the j-th indicator.

$$w_j = \frac{g_j}{\sum_{j=1}^{n} g_j}, j = 1, 2, \cdots, n \tag{16}$$

Where $g_j = 1 - e_j$ represents the information utility of the j-th indicator value. The larger the information entropy of the indicator, the less information it carries, and the smaller the information utility.

7) According to the objective weights obtained using the entropy weight method, the comprehensive score is calculated using the linear weighting method for overall operational quality

FIGURE 7
Field test implementation of the system.

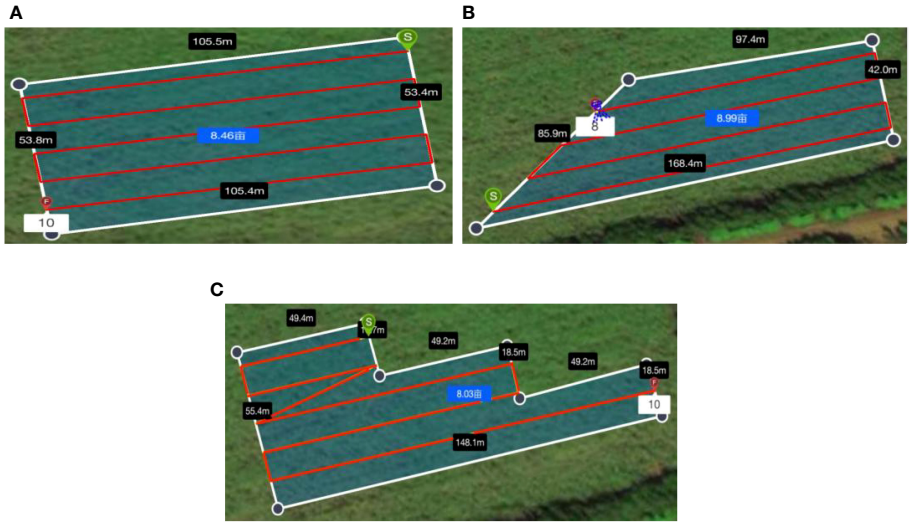

FIGURE 8
Schematic diagram of field plots in field experiments.

evaluation.

$$F_i = \sum_{j=1}^{n} w_j x_{ij}^{'}, i = 1, 2, \cdots, m; j = 1, 2, \cdots, n \quad (17)$$

3 Results and discussion

3.1 Ideal and actual delivery operational effects

In the ideal operational state, without considering factors such as flight route deviation, the ideal landing point diagram of the trichogramma ball is obtained. Using the center of the trichogramma ball's ideal landing point as the center of a circle d = 14.9 m, a schematic diagram of the coverage of the balls in three types of fields is drawn as shown in Figures 12A, C, E. The data is analyzed to obtain the ideal operational data in Table 4.

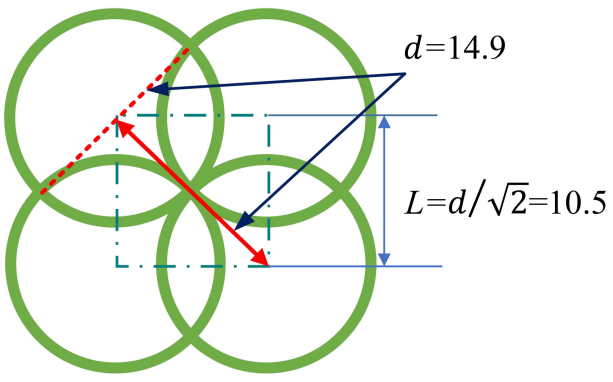

FIGURE 9
Trichogramma balls effect coverage area.

In the actual experimental field, the lush foliage of pineapple branches and the small size of the trichogramma ball make it very easy for falling balls to go unnoticed, resulting in a lack of actual landing points or redundant sampling due to previous missed detection. To avoid these situations affecting the experimental data, an average spacing is used as a reference, for obvious redundant landing points along the flight path, ideal ball landing points are used as reference points for deletion. for obvious missing points, including obvious missing points at the beginning or end of the route, the data is filled at an average spacing from the nearby reference point(the nearby actual landing point). Then With the landing point as the center of the circle d = 14.9m, a schematic diagram of the effective coverage area is drawn, as shown in Figure 13, which is simplified to Figures 12B, D, F. The actual operational parameters and performance indicators are also shown in Table 4. In terms of the uniqueness of the test results, as can be seen from Figures 12A, C, E, to ensure full coverage of the target area in rectangular, trapezoidal, and stepped fields, the flight path and release points are unique. Therefore, in the operation, the starting point of the UAV to begin to drop the trichogramma balls needs to be marked in advance in the flight control system.

From Table 4, it can be seen that in actual delivery operations, only the number of balls dropped in trapezoidal fields (50) reaches the ideal number of delivery operations (50), while rectangular (45) and stepped (37) fields do not achieve the same ideal number of delivery operations (50, 44), which will have an impact on the operational effect. In actual operations, the coverage rate of balls dropped can reach 97%, and the delivery area per unit time can reach 4158 m^2/min.

From the data in Table 4, the comparison chart of the five indicators obtained from three different boundary fields under ideal and actual operating conditions is shown in Figures 14 and 15, respectively. From Figures 14 and 15, it can be seen that in terms of the effective coverage rate η_1, in ideal situations, rectangle η_1 > trapezoidal η_1 > stepped η_1; in actual situations, trapezoidal η_1 >

FIGURE 10
Manual sampling of trichogramma ball drop points data.

rectangle η_1 > stepped η_1, stepped η_1 is always the smallest. The main reason is that the height of the ladder at the step is not up to the height standard of two trichogramma balls, when planning the path, it can only be covered by one trichogramma balls delivery route, and the number of pitches is minimum, which leads to the increase of the uncovered area of the operation and the decrease of the effective coverage rate η_1. For rectangular and trapezoidal fields, under ideal operational conditions, all four sides of the rectangular field are regular right-angled sides (90°), the positioning of the pitch points is planned so that the trichogramma balls can cover all routes and also cover all target area. For the trapezoidal field, at its hypotenuse, although the planned pitch point can cover all routes, it does not consider the difficult-to-cover gaps between upper and lower flight routes caused by the oblique edges, therefore, in the ideal situations, rectangle η_1 > trapezoidal η_1. In actual situations, trapezoidal η_1 > rectangle η_1, and compared to the ideal situations, the overall η_1 declined. The main reason for this is that during actual operations, deviations in drone flight paths and the landing positions of the trichogramma balls lead to a decline in the overall coverage effects. It is also found that during actual operations, the largest uncovered area is at the edges and corners of the field.

Theoretically, the relationship between the field edge angle θ and the uncovered area S at the edge corners satisfies Equation 18, and its relationship curve is shown in Figure 16 (when R=1). The schematic diagram is shown in Figure 17.

$$S = R^2\left[tan\frac{\pi-\theta}{2} - \frac{\pi-\theta}{2}\right] \quad (18)$$

As shown in Figure 16, with the increase of θ, the uncovered area decreases, and the circular area covered by the ball increasingly matches the edge boundaries. Relatively speaking, when θ > 90° (Figure 17A), the circular area covered by the ball is more fit with the boundary. The larger θ is, the higher the fit and the smaller the uncovered area are. When θ = 90° (Figure 17B), the circular area covered by the ball is difficult to fit with the boundary, and the uncovered area is larger than that when θ > 90°. When θ < 90° (Figure 17C), the circular area covered by the ball is the most difficult to fit with the boundary, and the uncovered area is larger than that when θ = 90°. Since the extension of the circular area covered by the balls beyond the field boundary does not bring about any damage similar to that after pesticide spraying, it only leads to an increase in the ineffective coverage area of the trichogramma balls.

Therefore, considering that the distance between the balls release point and the vertex of the edge and corner should be equal to that between the balls release point and vertex of edge and corner in Figure 17A), both are L (Figures 17A, D), so as to reduce the large uncovered area caused in Figure 17C. Therefore, in actual operations, this system can easily achieve a higher effective coverage rate η_1 in fields with θ > 90°, and the effective coverage rate η_1 is the lowest in stepped fields due to they have more right-angle edges.

Due to the fact that the sum of effective coverage rate η_1 and uncover rate η_2 is 1, the changes of η_1 and η_2 in the three types of fields exhibit an inverse synchronization relationship. Therefore, when quantifying the effectiveness of the operation, one of the changes is selected as an evaluation indicator. In this operational

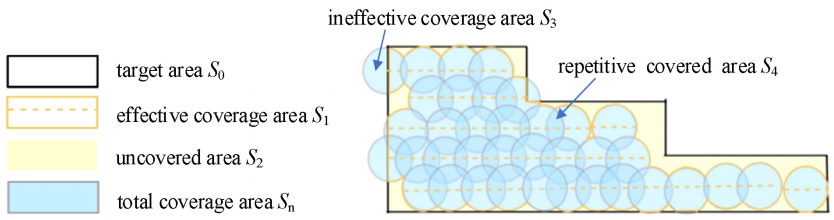

FIGURE 11
Schematic diagram of area indicators.

10.3389/fpls.2023.1247169

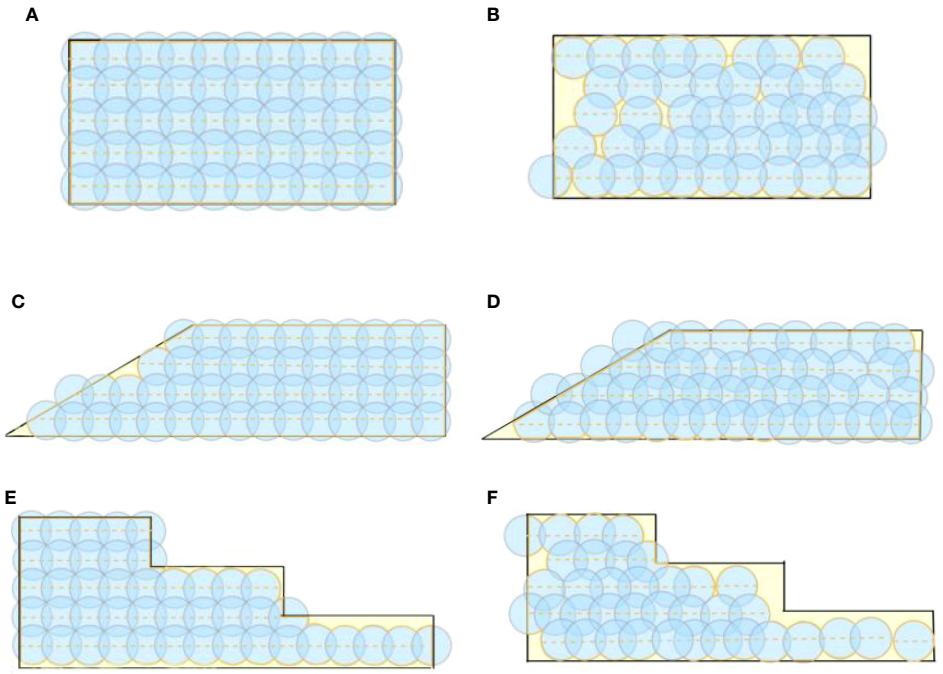

FIGURE 12
Schematic diagram of the trichogramma balls coverage range: **(A)** Ideal coverage diagram of rectangular fields, **(B)** Actual coverage diagram of rectangular fields, **(C)** Ideal coverage diagram of trapezoidal fields, **(D)** Actual coverage diagram of trapezoidal fields, **(E)** Ideal coverage diagram of stepped fields, **(F)** Actual coverage diagram of stepped fields.

quality evaluation system, the effective coverage rate η_1 is chosen as the system operational effect evaluation indicator.

In terms of the invalid coverage rate η_3, it is clear that the lower the η_3, the better the operation. From Figures 14 and 15, it can be seen that ideally, the stepped η_3< rectangle η_3< trapezoidal η_3. Actually, rectangle η_3<stepped η_3< trapezoidal η_3,with the trapezoid always being the largest, This is mainly due to that in order to improve the effective coverage area, the trapezoidal field

TABLE 4 Operational data of the trichogramma balls delivery system.

	Ideal Operation			Actual Operation		
	rectangle	trapezoidal	stepped	rectangle	trapezoidal	stepped
Number of pitches	50	50	44	45	50	37
S_n (m^2)	6030.16	6156.98	5522.14	5451.53	6209.67	4793.63
S_0 (m^2)	5565.00	5565.00	5565.00	5565.00	5565.00	5565.00
S_1 (m^2)	5564.11	5495.21	5135.73	5192.61	5419.44	4488.89
S_2 (m^2)	0	64.14	438.53	372.39	145.56	1076.11
S_3 (m^2)	465.16	656.10	251.84	258.92	776.13	303.20
S_4 (m^2)	2694.95	2568.13	2155.96	2401.07	2515.44	1662.95
η_1 (%)	99.98	98.74	92.28	93.31	97.38	80.66
η_2 (%)	0	1.15	7.88	6.69	2.61	19.33
η_3 (%)	8.36	11.79	4.52	4.65	13.94	5.45
η_4 (%)	92.27	88.33	88.29	89.16	85.46	76.49
η_5 (%)	44.69	41.71	39.04	44.04	40.51	34.69
Total pitching time (s)				125.00	125.80	126.20
Area delivered per unit time (m^2/min)				3766.39	4158.27	3067.36

10.3389/fpls.2023.1247169

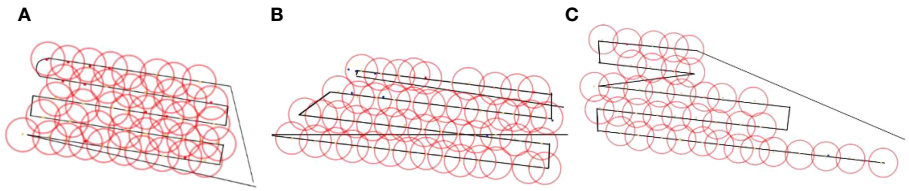

FIGURE 13
Schematic diagram of the actual coverage range: **(A)** Rectangular field, **(B)** Trapezoidal field, **(C)** Stepped field.

adds the dropping point of the balls at the hypotenuse, thereby increasing the ineffective coverage area outside the target area. In ideal situations, stepped η_3 < rectangle η_3, mainly because the stepped field's step height is less than the height required to put two balls, therefore, only one row of delivery points is planned, so that the invalid coverage area S_3 is reduced. In actual situations, the rectangle η_3 < stepped η_3, mainly due to the deviation of the route and the position of the landing point at the right angle turning point, and at the right angle corners, this deviation is more pronounced, such as the stepped shape has multiple right angle corners, resulting in a greater pitch deviation and resulting in a smaller effective coverage area and a larger ineffective coverage area. However, ineffective coverage for the balls delivery operation does not lead to pesticide drift into invalid coverage areas as when spraying pesticides, so the influence of η_3 can be weakened or even not considered in the evaluation process. The effectiveness of ineffective coverage is indirectly reflected by the utilization rate η_4, obviously, the higher the better. Under ideal and actual operating conditions, all are rectangular η_4 > trapezoidal η_4 > stepped η_4, but in terms of the balls repetition rate η_5, obviously the lower the better. Under ideal and actual operating conditions, all are stepped η_5 < trapezoidal η_5 < rectangular η_5, so it is difficult to simply judge which type of field is the best from the trichogramma balls utilization effect.

3.2 Analysis of operational quality evaluation

To quantify the differences in operational quality among three shapes of fields in ideal and actual delivery operations, we set up a comprehensive evaluation system for operational quality, It quantitatively analyzes from two aspects: the effectiveness of field operation U_1 and the utilization effect of trichogramma balls U_2. The aforementioned evaluation indicators are divided into two levels. The effective coverage rate η_1 reflects the system operational effect U_1, while the balls utilization rate η_4 and repetition rate η_5 reflect the trichogramma balls utilization effect U_2. The specific grading is shown in Table 5.

Firstly, the entropy weight method is used to determine the secondary indicator weights of η_4 and η_5 to evaluate the utilization effect of trichogramma balls. The trichogramma balls utilization rate η_4 is a positive effect indicator, the larger the indicator, the better the utilization effect of balls, which can be directly standardized using Equation 8. The repetition rate of the balls η_5 is a negative effect indicator, the larger the indicator, the worse the utilization effect of balls, which should be converted into a positive effect indicator using Equation 9 to obtain the standardized matrix X_1. Then, after translation processing using Equation 10, the proportion matrix P_1 of η_4, η_5 is calculated according to Equation 11 for evaluating different fields, and the information entropy matrix E_1 of η_4, η_5 is calculated according to Equation 12, the weight matrix W_1 of η_4, η_5 is calculated according to Equation 13. The linear weighting method of Equation 14 is used to calculate the data of trichogramma balls utilization effect U_2, and then the same method is used to determine the X_2, P_2, E_2, and W_2 of the two primary indicators U_1, U_2,The specific data obtained under ideal and actual conditions are as follows, and the indicator weights are shown in Table 5. The comprehensive field operational scores of three types of field blocks under ideal and actual conditions are obtained by using the linear weighting method with weights and standardized sample values, and the data are shown in Figure 18.

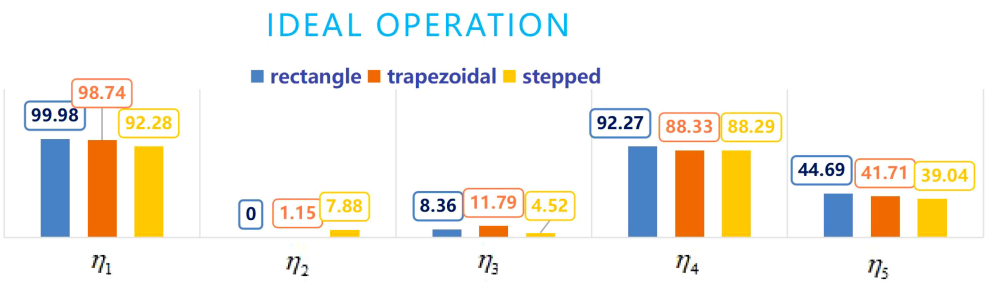

FIGURE 14
Comparison chart of five indicators for three fields under ideal operating conditions.

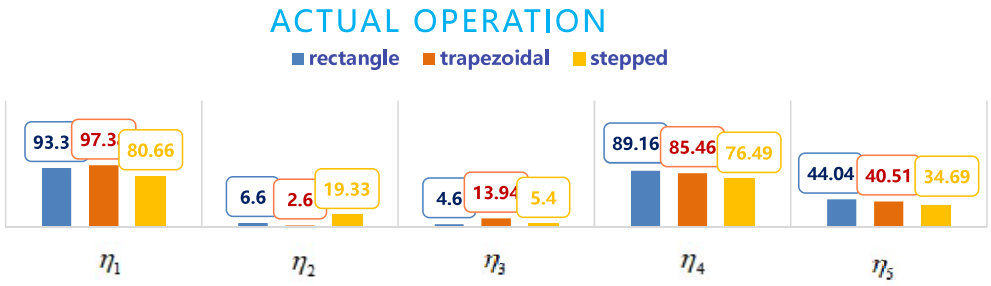

FIGURE 15
Comparison chart of five indicators for three fields under actual operating conditions.

$$X_{1ideal} = \begin{bmatrix} 1.0000 & 0.0000 \\ 0.0101 & 0.5274 \\ 0.0000 & 1.0000 \end{bmatrix} \quad P_{1ideal} = \begin{bmatrix} 0.9881 & 0.0007 \\ 0.0109 & 0.3453 \\ 0.0010 & 0.6541 \end{bmatrix} \quad E_{1ideal} = [0.0618 \ 0.5913]$$

$$X_{2ideal} = \begin{bmatrix} 1.0000 & 1.0000 \\ 0.8390 & 0.0000 \\ 0.0000 & 0.2576 \end{bmatrix} \quad P_{2ideal} = \begin{bmatrix} 0.5434 & 0.7941 \\ 0.4560 & 0.0007 \\ 0.0005 & 0.2051 \end{bmatrix} \quad E_{2ideal} = [0.6313 \ 0.4676]$$

$$X_{1actual} = \begin{bmatrix} 1.0000 & 0.0000 \\ 0.7080 & 0.3775 \\ 0.0000 & 1.0000 \end{bmatrix} \quad P_{1actual} = \begin{bmatrix} 0.5850 & 0.0007 \\ 0.4144 & 0.2741 \\ 0.0006 & 0.7251 \end{bmatrix} \quad E_{1actual} = [0.6217 \ 0.5399]$$

$$X_{2actual} = \begin{bmatrix} 0.7566 & 0.0000 \\ 1.0000 & 0.7228 \\ 0.0000 & 1.0000 \end{bmatrix} \quad P_{2actual} = \begin{bmatrix} 0.4305 & 0.0006 \\ 0.5689 & 0.4357 \\ 0.0006 & 0.5637 \end{bmatrix} \quad E_{2actual} = [0.6262 \ 0.6274]$$

From Figure 18, it can be seen that from the perspective of system field comprehensive operational quality evaluation, under ideal operational conditions, the comprehensive operational quality score F of rectangular fields is the highest, reaching 1.000, while under actual operational conditions, the comprehensive operational quality score F of trapezoidal fields is the highest, at 0.8866. This indicates that in actual operations, if any complex boundary natural fields are decomposed into several rectangular, trapezoidal, or stepped small fields, the more trapezoidal small fields, the higher the comprehensive operational quality of this complex boundary field.

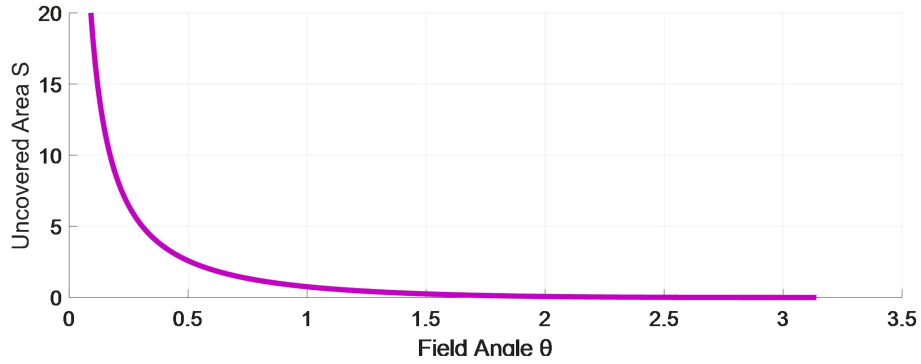

FIGURE 16
Relationship Curve between Field Angle θ and Uncovered Area S.

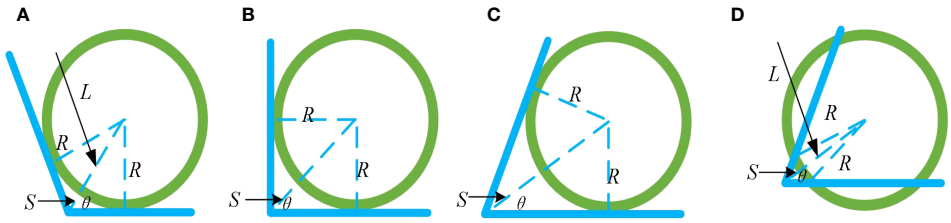

FIGURE 17
Diagram of the fit relationship between edges and circles: **(A–D)**.

10.3389/fpls.2023.1247169

TABLE 5 Comprehensive evaluation indicators and weights of operational quality.

primary indicators	weight (W)		secondary indicators	weight (W)	
Field operational effect (U_1)	ideal	0.4092	η_1	ideal	0.4092
				actual	0.5008
	actual	0.5008	η_2	ideal	0
				actual	0
Trichogramma balls utilization effect (U_2)	ideal	0.5908	η_3	ideal	0
				actual	0
			η_4	ideal	0.6966
	actual	0.4992		actual	0.4512
			η_5	ideal	0.3034
				actual	0.5488

4 Conclusion

The initial use of chemical pesticides can effectively control pests, but long-term or excessive use of chemical pesticides can cause pollution of the atmosphere and soil, as well as harm to human health. Studies have shown that using natural enemies for biological pest control presents significant potential and can overcome the problems associated with chemical pesticide control. The introduction of trichogramma is currently a prevalent method of biological pest control. The deployment of trichogramma balls by UAVs can operate in various complex environments, offering advantages such as higher efficiency, faster speed, reduced costs, less waste, and fewer labor resources. However, current research on the trichogramma balls delivery system is still in its nascent stages. Especially when operating in fields with complex boundaries, the reliability and accuracy of this method need improvement, and the evaluation indicators for its effectiveness also need to be clarified. These issues are studied in this article. The experiment shows that the pitching accuracy of the trichogramma balls delivery system designed in this article exceeds 97.69%, and all loaded balls are released without any issues of stuck balls or missed releases, indicating that the system is accurate and reliable. The efficiency of the system can reach 4158 m^2/min, and the coverage rate of trichogramma balls can exceed 97%.

In order to comprehensively evaluate the actual delivery effect of UAVs, the effective coverage rate η_1, uncover rate η_2, ineffective coverage rate η_3, utilization rate of balls η_4, and repetition rate of balls η_5 are defined this article. Since the sum of η_1 and η_2 is 1, the changes of η_1 and η_2 in the exhibit an inverse synchronization relationship. So when quantifying the effectiveness of the operation, η_1 is chosen as the system operational effect evaluation indicator; η_3 reflects the degree of coverage of the balls beyond the boundary, even though there may be cases of balls coverage area exceeding the boundary, it will not cause drug damage like that caused by pesticide overreach spraying, so the impact of η_3 is not considered in the evaluation process, the ineffective coverage situation is indirectly reflected by the utilization rate of balls η_4, so η_4 and η_5 are used to evaluate the utilization effect of balls. The weight of each indicator is determined by the two-level indicator weighting method, and through linear weighting method, a comprehensive score is obtained to analyze the overall operational quality of the trichogramma balls UAV delivery system. this method provides a standard for a comprehensive and objective evaluation of the overall operational quality of the

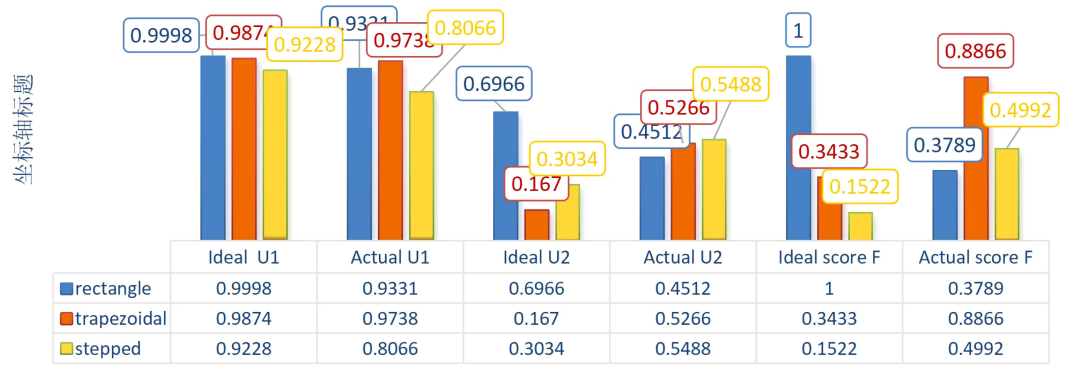

	Ideal U1	Actual U1	Ideal U2	Actual U2	Ideal score F	Actual score F
rectangle	0.9998	0.9331	0.6966	0.4512	1	0.3789
trapezoidal	0.9874	0.9738	0.167	0.5266	0.3433	0.8866
stepped	0.9228	0.8066	0.3034	0.5488	0.1522	0.4992

FIGURE 18
Comprehensive operational quality evaluation data of the three types of boundary fields.

trichogramma balls UAV delivery system, and the defined indicators provide target parameters for the flight path planning of the trichogramma balls UAV delivery system.

The analysis of the system field operational effect reveals that a larger obtuse edge in the actual operational field boundary can result in a higher effective coverage area, at the right angle edge equal to 90°, it is easy to lead to less effective coverage area, and the more right angle edge, the less effective coverage area, and at the sharp angle edge less than 90°, the effective coverage area is increased when the ball drop point is pushed to the apex of the acute angle, because ineffective coverage of biological control does not lead to ecological deterioration, so the effect of the resulting high ineffective coverage is weakened in the comprehensive evaluation. Therefore, among the rectangular, trapezoidal and stepped fields, the trapezoidal fields operational effect is the best, followed by rectangular fields, and stepped fields operational effect is the worst. When comprehensively evaluating the effect of field operations and the utilization effect of balls, according to the scoring results, the comprehensive operational quality of the trapezoidal fields is the best, followed by the stepped, and the rectangular is the worst. In summary, it is better to divide the fields boundaries into trapezoids wherever possible when the UAV is operating in the area. This can achieve the best operating effect.

The employment of UAVs for the delivery of trichogramma balls to control insect pests has led to a reduction in pesticide usage, even in cases of redelivery or cross-border delivery, This method does not cause drug damage, thereby substantially enhancing the overall ecological benefits (Markle et al., 2016; Tang et al., 2018; Richardson et al., 2020; Fu et al., 2021; Li et al., 2021; Yan et al., 2021). The research conducted on this method and the evaluation indicators used to assess its operational effect have both provided technical support and a scientific basis for its application and promotion. This contributes to ecological protection in the agricultural field and the development of high-quality agriculture. Future work will focus on the path planning, flight route control, and factors affecting landing position during the UAV delivery process to achieve a higher operational quality and more precise pest control effects.

Data availability statement

The original contributions presented in the study are included in the article/Supplementary Material. Further inquiries can be directed to the corresponding author.

Author contributions

JLi contributed to conception and design of the study. ML and YQ organized the database. HX, ML, YQ, GF, YZ and JLv performed the statistical analysis. HX, ML, and YQ wrote the first draft of the manuscript. HX, ML, YQ, GF, YZ, and JLi wrote sections of the manuscript. All authors contributed to the article and approved the submitted version.

Funding

The author(s) declare financial support was received for the research, authorship, and/or publication of this article. The study was funded by the Guangdong Basic and Applied Basic Research Foundation (2023A1515011932), Guangzhou key research and development project (202206010164&2023B03J1323), Technology R&D Project (H20210985).

Conflict of interest

The authors declare that the research was conducted in the absence of any commercial or financial relationships that could be construed as a potential conflict of interest.

Publisher's note

All claims expressed in this article are solely those of the authors and do not necessarily represent those of their affiliated organizations, or those of the publisher, the editors and the reviewers. Any product that may be evaluated in this article, or claim that may be made by its manufacturer, is not guaranteed or endorsed by the publisher.

Supplementary material

The Supplementary Material for this article can be found online at: https://www.frontiersin.org/articles/10.3389/fpls.2023.1247169/full#supplementary-material

References

Babendreier, D., Wan, M., Tang, R., Gu, R., Tambo, J., Liu, Z., et al. (2019). Impact assessment of biological control-based integrated pest management in rice and maize in the greater mekong subregion. *Insects* 10 (8), 226. doi: 10.3390/insects10080226

Bzowska-Bakalarz, M., Bulak, P., Beres, P. K., Czarnigowska, A., Czarnigowski, J., Karamon, B., et al. (2020). Using gyroplane for application of Trichogramma spp. against the European corn borer in maize. *Pest Manage Sci.* 76 (6), 2243–2250. doi: 10.1002/ps.5762

Cao, G., Li, Y., Nan, F., Liu, D., Chen, C., and Zhang, J. (2020). Development and analysis of plant protection UAV flight control system and route planning research. *Trans. Chin. Soc. Agric. Mach.* 51 (08), 1–16. doi: 10.6041/j.issn.1000-1298.2020.08.001

Chen, S., Wu, C., Chen, L., Chang, K., Qian, S. Q., Chen, W., et al. (2020). Design and test of aerial broadcast device for agricultural granular materials. *Int. J. Precis Agric. Aviat* 3 (4), 44–50. doi: 10.33440/j.ijpaa.20200304.133

Cheng, J., and Zhu, Z. (2017). Development of rice pest management in the past 60 years in China:problems and strategies. *J. Plant Protection.* 44 (6), 885–895. doi: 10.13802/j.cnki.zwbhxb.2017.2017901

Ding, N., Li, H., Yan, A., Liu, P., Han, L., and Wei, W. (2021). Optimization and experiment on straw multi-stage continuous cold roll forming for molding parameters. *Trans. Chin. Soc. Agric. Mach.* 52 (10), 196–202+290. doi: 10.6041/j.issn.1000-1298.2021.10.020

Dionne, A., Khelifi, M., Todorova, S. I., and Boivin, G. (2018). Design and Testing of a Boom Sprayer Prototype to Release Trichogramma ostriniae (Hymenoptera: Trichogrammatidae) in Sweet Corn for Biocontrol of Ostrinia nubilalis (Hübner) (Lepidoptera: Crambidae). *Trans. ASABE* 61, 1867–1879. doi: 10.13031/trans.12922

Fang, G., Bi, J., Li, C., Yue, L., Li, X., Liu, J., et al. (2022). Evaluation of the comprehensive quality of sea buckthorn fruit in four areas of China. *Trans. Chin. Soc. Agric. Eng.* 38 (21), 249–260. doi: 10.11975/j.issn.1002-6819.2022.21.029

Fu, R., Chen, C., Wang, J., Chen, X., and Lu, D. (2021). Control conditions and effects of plant protection unmanned aerial vehicle (UAV) on diseases and insect pests of rice. *J. Agric. Sci. Technol.* 23 (04), 103–109. doi: 10.13304/j.nykjdb.2019.0682

Gauthier, P., Khelifi, M., Dionne, A., and Todorova, S. (2019). Technical feasibility of spraying trichogramma ostriniae pupae to control the european corn borer in sweet corn crops. *Appl. Eng. Agric.* 35 (2), 185–192. doi: 10.13031/aea.12833

Giles, D. K., Gardner, J., and Studer, H. E. (1995). Mechanical release of predacious mites for biological pest control in strawberries. *Trans. ASAE* 38 (5), 1289–1296. doi: 10.13031/2013.27950

Herren, H., Bird, T. J., and Nadel, D. J. (1987). Technology for automated aerial release of natural enemies of the cassava mealybug and cassava green mite. *Int. J. Trop. Insect Sci.* 8, 883–885. doi: 10.1017/S1742758400023122

Iost, F. H., Heldens, W. B., Kong, Z. D., and de Lange, E. S. (2020). Drones: innovative technology for use in precision pest management. *J. Economic Entomology* 113 (1), 1–25. doi: 10.1093/jee/toz268

Ji, S., Gong, J., Cui, K., Zhang, Y., and Mostafa, K. (2022). Performance test and parameter optimization of trichogramma delivery system. *Micromachines* 13 (11), 1–10. doi: 10.3390/mi13111996

Kumar, K. K., and Arthurs, S. (2021). Recent advances in the biological control of citrus nematodes: A review. *Biol. Control* 157, 104593. doi: 10.1016/j.biocontrol.2021.104593

Li, D., Yuan, X., Zhang, B., Zhao, Y., Song, Z., and Zou, C. (2013). Report of using unmanned aerial vehicle to release trichogramma. *Chin. J. Biol. Control* 29 (3), 455–458. doi: 10.16409/j.cnki.2095-039x.2013.03.020

Li, X., Giles, D. K., Niederholzer, F. J., Andaloro, J. T., Lang, E. B., and Watson, L. J. (2021). Evaluation of an unmanned aerial vehicle as a new method of pesticide application for almond crop protection. *Pest Manage Sci.* 77 (1), 527–537. doi: 10.1002/ps.6052

Markle, J. C., Niederholzer, F. J. A., and Zalom, F. G. (2016). Evaluation of spray application methods for navel orangeworm control in almonds. *Pest Manag Sci.* 72 (12), 2339–2346. doi: 10.1002/ps.4279

Martel, V., Johns, R. C., Jochems-Tanguay, L., Jean, F., Maltais, A., Trudeau, S., et al. (2021). The use of UAS to release the egg parasitoid trichogramma spp. (Hymenoptera: trichogrammatidae) against an agricultural and a forest pest in Canada. *J. Econ. Entomol.* 114, 5, 1867–1881. doi: 10.1093/jee/toaa325

Parra, J. R. P. (2014). Biological control in Brazil: an overview. *Scientia Agricola* 71, 420–429. doi: 10.1590/0103-9016-2014-0167

Qin, Y., Lyu, G., Guan, K., and Zhou, H. (2023). Durability assessment and life prediction of concrete by entropy weight method. *J. Chin. Ceram Soc.* 51 (05), 1–11. doi: 10.14062/j.issn.0454-5648.20220694

Richardson, B., Rolando, C. A., Somchit, C., Dunker, C., Strand, T. M., and Kimberley, M. O. (2020). Swath pattern analysis from a multi-rotor unmanned aerial vehicle configured for pesticide application. *Pest Manage Sci.* 76 (4), 1282–1290. doi: 10.1002/ps.5638

Tang, Y., Hou, C., Luo, S., Lin, J., Yang, Z., and Huang, W. (2018). Effects of operation height and tree shape on droplet deposition in citrus trees using an unmanned aerial vehicle. *Comput. Electron Agric.* 148, 1–7. doi: 10.1016/j.compag.2018.02.026

Wang, Z., Cheng, X., Xie, Y., Hong, C., Hu, M., Gao, Y., et al. (2022). Effects of different water and fertilizer use patterns on the lodging resistances of indica and japonica rice. *Trans. Chin. Soc. Agric. Eng.* 38 (09), 108–118. doi: 10.11975/j.issn.1002-6819.2022.09.012

Wang, Z., Liu, Y., Shi, M., Huang, J., and Chen, X. (2019). Parasitoid wasps as effective biological control agents. *J. Integr. Agric.* 18, 705–715. doi: 10.1016/S2095-3119(18)62078-7

Xu, D., Bai, Y., Gong, X., and Xu, Z. (2016). Design of Trichogramma delivering system based on hex-rotor UAV. *Trans. Chin. Soc. Agric. Mach.* 47 (01), 1–7. doi: 10.6041/j.issn.1000-1298.2016.01.001

Yan, X., Shi, X., Liu, X., Du, Y., Yang, D., and Yuan, H. (2021). The spray drift risk of plant protection unmanned aerial vehicle (UAV) spraying neonicotinoid pesticides to honey bees. *J. Plant Prot.* 48 (03), 477–482. doi: 10.13802/j.cnki.zwbhxb.2021.2021836

Yang, S., Zheng, Y., and Liu, X. (2019). Research status and trends of downwash airflow of spray UAVs in agriculture. *Int. J. Precis. Agric. Aviation* 2 (1), 1–8. doi: 10.33440/j.ijpaa.20190201.0023

Zang, L., Wang, S., Zhang, F., and Desneux, N. (2021). Biological control with Trichogramma in China: History, present status, and perspectives. *Annu. Rev. Entomol* 66, 463–484. doi: 10.1146/annurev-ento-060120-091620

Zhan, Y., Chen, S., Wang, G., Fu, J., and Lan, Y. (2021). Biological control technology and application based on agricultural unmanned aerial vehicle (UAV) intelligent delivery of insect natural enemies (Trichogramma) carrier. *Pest Manage Sci.* 77 (7), 3259–3272. doi: 10.1002/ps.6371